

# Delay Differential Neoclassical Growth Model\*

Akio Matsumoto<sup>†</sup>  
Chuo University

Ferenc Szidarovszky<sup>‡</sup>  
University of Arizona

## Abstract

This paper develops a continuous-time neoclassical growth model with time delay. Despite of its simple structure, the resulting dynamic system shows emergence of erratic fluctuations in the capital accumulation process when the production function is unimodal and the delay in production is explicitly considered. It complements the seminal paper of Day (1982) in which a discrete-time neoclassical growth model displayed chaotic behavior for some configurations of the propensity to save, the growth rate of labor and the capital depreciation rate. Our analysis has at least two implications. First, nonlinearities and delay matter for a birth of aperiodic fluctuations of national product in the continuous-time model. Second, comparing the effects caused by two different time delays, fixed and continuously distributed time delays, reveals that the continuous-time model with the former can generate complex fluctuations while the one with the latter generates simple fluctuations when the shape parameter of the density function is small and complex fluctuations when large.

**Keyword:** Neoclassical growth model, continuously distributed time delay, fixed time delay, complex dynamics, period-doubling bifurcation

**JEL:** E13, E32, C62

---

\*The authors highly appreciate financial supports from the Japan Society for the Promotion of Science (Grant-in-Aid for Scientific Research (C) 21530172), Chuo University (Joint Research Grant 0981) and the Japan Economic Research Foundation. They are also grateful to K. Ishiyama and M. Kobayashi for their supporting computational studies. The paper was prepared when the second author visited the Department of Science and Engineering of Chuo University. He appreciated its hospitality over his stay. The usual disclaimer applies.

<sup>†</sup>Department of Economics, Chuo University, 742-1, Higashi-Nakano, Tokyo, 192-0393, Japan. akiom@tamacc.chuo-u.ac.jp +81-426-74-3351 (tel); +81-426-74-3452 (fax)

<sup>‡</sup>Department of Systems and Industrial Engineering, University of Arizona, Tucson, AZ, 85721-0020, USA. szidar@sie.arizona.edu; +1-520-621-6557 (tel); +1-520-621-6555 (fax).

# 1 Introduction

In his seminal papers, Day (1982, 1983) examines two conventional dynamic models, one of neoclassical economic growth and the other of productivity and population growth, to show emergence of complex behavior from a quite simple economic structure when sufficient nonlinearities are present. Both models are constructed in discrete-time and have the mound-shaped production function representing the negative effects of pollution caused by increasing capital. It is then analytically and numerically demonstrated that the models generate not only periodic cycles but also chaotic behavior for certain values of the shape parameter of the production function. Each paper has been one of the most influential papers in the study of nonlinear economic dynamics for the last three decades. Since the publications of these papers, a lot of efforts have been devoted to deepen the understanding of economic complexity including chaotic behavior, multistability, basins of attractions and so on. Overviews of early contributions and recent developments in nonlinear economic dynamics are found in, to name a few, Day (1994), Puu (2003) and Bischi *et al.* (2010).

In discrete-time analysis, there is a clear and simple criteria such as the "period-three condition" of Li and Yorke (1975) to detect chaos, which can be applied to first-order nonlinear difference equations. In consequence, discrete-time chaos has numerous applications to economic models, as shown, for example, in the papers collected in Rosser (2004). On the other hand, the economic applications of continuous-time chaos are so far limited. This may be due to the facts that there are no general criteria to establish the presence of chaos in continuous-time analysis and that a continuous-time system must be at least three dimensional. As a result, advanced analytical and numerical considerations are required to find chaos in continuous models.

Despite of this inconvenience, this paper aims to reconsider emergence of erratic and unstable fluctuations in a delay continuous-time neoclassical growth model with the following four reasons. The first reason is concerned with continuous time scales and is due to Gandolfo (1997) who raises a question on the choice of continuous or discrete time scales in the construction of dynamic models and gives eight reasons to be in favor of the use of continuous models including the following: it is natural to treat economic phenomena as continuous, provided that the variables to be examined in the dynamic models are the outcomes of a great number of decisions taken by different agents at different points of time. This is in particular a case in the aggregate model. The second is concerned with a delay in production process. In the cases of most models discussed earlier in the literature, it is assumed that each economic agents has instantaneous information about its own as well as its rivals' behavior. This assumption has mathematical convenience but does not fully describe real economic situations in which there are always time delays between the times when information obtained and the times when the decisions are implemented. The third is concerned with nonlinearities. If the analysis is confined to a neighborhood of a stationary point, then linear systems are appropriate. However if certain "global" phenomenon is considered, then nonlinear behavior is responsible for the endogenous dynamics. Finally the fourth reason is concerned with the use of the neoclassical model and similar to the argument of Day (1983). Namely, it has the simplest possible framework and still provides a convenient starting point for an investigation of continuous complex dynamics. In addition

to these, we have an academic curiosity to find economic circumstances under which continuous models give rise to similar dynamic behavior as discrete models. Similarly to the spirit and function form of the discrete-time neoclassical model of Day (1982), continuous time scales, nonlinearity and delay are assumed in this paper.

The structure of the paper is as follows. Section 2 gives a brief overview of the neoclassical growth model and discusses the fact that the model is globally stable if its dynamics is constructed in continuous time while the discrete-time model possesses the possibility of chaotic outcomes when the stationary state is locally unstable. The continuous-time neoclassical growth model can be transformed into a delay differential system which is also capable of producing complex dynamics. Section 3 introduces continuously distributed time delay and Section 4 replaces it with fixed time delay. Section 5 compares the effects caused by these two different types of delays. Finally some concluding remarks are given in Section 6.

## 2 Neoclassical Growth Model

This section serves as a short summary of the neoclassical aggregate model of growth, which can be traced back to Solow (1956) and Swan (1956). An enormous amount of work carried out since then. The main interest has been on two questions: whether full employment growth is possible and whether such growth is stable. Affirmative answers are given under various conditions. The turning point is Day's (1982) model showing the occurrence of chaos.

This section is divided into two parts: First the continuous-time version is briefly discussed to show asymptotic stability of the steady state and then the discrete-time version is abstracted. Erratic fluctuations are demonstrated when the steady state is locally unstable and the production function involves strong nonlinearities.

### 2.1 Continuous Time Scales

In its simplest version, the neoclassical growth model assumes that the economy has one sector producing national product  $Y$  with a production function,

$$Y(t) = F(L(t), K(t)) \quad (1)$$

where  $L(t)$  is labor,  $K(t)$  is capital and  $t$  denotes time.  $F$  is assumed to be conventional implying that it is constant returns to scale (i.e.,  $F(\alpha L, \alpha K) = \alpha F(L, K)$  for  $\alpha > 0$ ) and the two factors are indispensable for production (i.e.,  $L(t) > 0$  and  $K(t) > 0$ ). Denoting consumption by  $C(t)$  and investment by  $I(t)$ , the equilibrium in the output market is described by the supply-equals-demand relation

$$Y(t) = C(t) + I(t). \quad (2)$$

We assume that the amount of consumption is a constant fraction of net income,

$$C(t) = (1 - s)(Y(t) - \mu K(t)) \quad (3)$$

where  $s \in (0, 1)$  is the average propensity to save and  $\mu \in (0, 1]$  is the depreciation ratio of capital. There are two sources of dynamics: investment and labor

supply. The amount of gross investment  $I(t)$  is equal to the sum of the change in capital stock and the amount of capital depreciation at each instant of time,

$$I(t) = \dot{K}(t) + \mu K(t), \quad (4)$$

where the dot over variables denotes time derivatives, e.g.,  $\dot{K}(t) = dK(t)/dt$ . We further assume that labor grows at a (exogenously determined) positive constant rate  $n > 0$ ,

$$L(t) = L_0 e^{nt} \quad (5)$$

where  $L_0$  is the amount of labor available at  $t = 0$ .

Substituting equations (1) and (4) into (2) gives

$$F(L(t), K(t)) = C(t) + \dot{K}(t) + \mu K(t).$$

Dividing both sides by  $L(t) > 0$  and introducing the per-capita variables,  $c(t) = C(t)/L(t)$  and  $k(t) = K(t)/L(t)$ , we obtain

$$f(k(t)) = c(t) + \frac{\dot{K}(t)}{L(t)} + \mu k(t) \quad (6)$$

where the assumption of constant returns to scale implies that we can write the production function in the "intensive" or "per-capita" form

$$f(k) = F\left(1, \frac{K}{L}\right).$$

Dividing both sides of equation (3) by  $L(t)$  gives

$$c(t) = (1 - s)(f(k(t)) - \mu k(t)).$$

Differentiating  $k(t)$  with respect to  $t$  and noticing that the growth rate of labor is  $n$ , we obtain, after arranging terms,

$$\frac{\dot{K}(t)}{L(t)} = \dot{k}(t) + nk(t).$$

Combining the last two equations with (6), we have the fundamental dynamic equation of the neoclassical aggregate growth model:

$$\dot{k}(t) = sf(k(t)) - \delta k(t) \text{ where } \delta = n + s\mu. \quad (7)$$

We now impose the conventional assumptions (i.e., Inada conditions) on the per-capita production function  $f(k)$ :

**Assumption 1.**

- (1)  $f'(k) > 0$  and  $f''(k) < 0$  for all  $k \geq 0$ ;
- (2)  $f(0) = 0$ ;
- (3)  $\lim_{k \rightarrow 0} f'(k) = \infty$  and  $\lim_{k \rightarrow \infty} f'(k) = 0$ .

Under these conditions, the continuous-time neoclassical growth model (7) has a steady state  $k^* > 0$  which is the unique positive solution of equation

$$sf(k^*) = \delta k^*.$$

Outside this steady state we have two possibilities:

$$\dot{k} > 0 \text{ for } k_0 < k^* \text{ or } \dot{k} < 0 \text{ for } k_0 > k^* \quad (8)$$

with  $k_0 \neq k^*$  and  $k_0 \neq 0$ . The directions of inequalities of  $\dot{k}$  in (8) imply the local asymptotical stability of the positive steady state. This classical result is well known from the literature.

## 2.2 Discrete Time Scales

In this section, we transform the continuous model to the discrete time model where  $t$  now refers to period  $t$ . The behavioral specifications (1), (2) and (3) are not affected by changing time scales. On the other hand, dynamic specifications (4) and (5) should be modified accordingly. The labor supply equation is changed to

$$L(t) = (1 + n)^t L_0 \quad (9)$$

where the notation  $n$  is used to denote the growth rate of labor. A law of motion for the capital stock in discrete time is obtained by replacing  $\dot{K}(t)$  in equation (4) by  $K(t + 1) - K(t)$ , so

$$K(t + 1) - K(t) = I(t) - \mu K(t). \quad (10)$$

Substituting (3) and (10) into the equilibrium relation (2) and re-arranging terms yield

$$sY(t) = K(t + 1) - (1 - s\mu)K(t).$$

Dividing both sides by  $L(t)$  and using relations  $y(t) = f(k(t))$  and  $L(t + 1)/L(t) = 1 + n$  yield the discrete-time fundamental dynamic equation of capital:

$$k(t + 1) = \frac{1}{1 + n} (sf(k(t)) + (1 - s\mu)k(t)) \equiv g(k(t)). \quad (11)$$

Given the initial condition  $k_0$ , this first-order difference equation determines the entire time path of the capital stock. The conventional neoclassical assumptions (i.e., Assumption 1) ensures that there is a positive and stable steady state  $k_s > 0$  such that  $k_s = g(k_s)$  and all trajectories monotonically converge to  $k_s$  as  $t \rightarrow \infty$  for all  $k_0 > 0$ . As a benchmark, given the well known Cobb-Douglas production function  $F(L, K) = AK^a L^{1-a}$  with  $A > 0$  being the technology parameter and  $a \in (0, 1)$ , the elasticity parameter, we have its intensive form  $f(k) = Ak^a$ . In this case it can be confirmed that the steady state is  $k_s = [sA/(n + s\mu)]^{1/(1-a)}$  which is locally asymptotically stable.

Day (1982) reconstructs this neoclassical theory of capital accumulation under circumstances in which productivity of the production function is reduced by a pollution effect caused by increasing concentration of capital. Applying the nonlinear dynamic theory, he demonstrates that erratic behavior exhibiting wandering and sawtooth patterns can emerge when sufficient nonlinearities are

present. In particular, in contrast to the conventional neoclassical assumptions, the per-capita production function is modified to have the form

$$f(k) = Ak^a(1 - k)^b \quad (12)$$

with  $A > 0$  and  $f'(k) < 0$  for large  $k$ . The factor  $(1 - k)^b$  reflects the influence of pollution on per-capita output. When the capital intensity increases, pollution increases as well. However for a small enough value of  $b$ , the pollution effect is so small that the modified production function behaves like the conventional production function. When  $b$  is relatively large, the pollution effect reduces national output. Substituting the new production function into (11), we have the modified fundamental equation of capital accumulation:

$$k(t+1) = \frac{sA}{1+n}k(t)^a(1 - k(t))^b + \frac{1 - s\mu}{1+n}k(t).$$

Consider a simplification by assuming that  $a = b = 1$ . Introducing the new variable  $z = Bk$  with

$$B = \frac{sA}{1 + (A - \mu)s}$$

reduces the fundamental equation to the logistic map,

$$z(t+1) = \theta z(t)(1 - z(t)) \quad (13)$$

where

$$\theta = \frac{1 + (A - \mu)s}{1 + n}.$$

A positive fixed point

$$z_s = \frac{\theta - 1}{\theta},$$

is obtained for  $\theta > 1$ . The dynamics of  $k(t)$  generated by (11) with the modified production function is equivalent to the dynamics of  $z(t)$  generated by the logistic map (13). The dynamic structure of (13) has been extensively studied and it is now well-known that equation (13) can generate a wide variety of dynamics ranging from monotonic convergence to chaotic behavior, depending on the value of  $\theta$ . The factor  $\theta$  usually varies between zero and four. In summary, the discrete-time neoclassical growth model (13) can generate the following dynamics:

- (1) monotonic convergence to zero for  $0 < \theta \leq 1$ ,
- (2) monotonic growth and convergence to  $z_s$  for  $1 < \theta \leq 2$ ,
- (3) oscillatory convergence to  $z_s$  for  $2 < \theta \leq 3$ ,
- (4) continued oscillations around  $z_s$  for  $3 < \theta \leq 4$ .

### 3 Growth Model with Continuously Distributed Time Delay

It is demonstrated in the first half of the last section that the continuous-time neoclassical growth model is definitely stable. It is also demonstrated in the latter half that the discrete-time neoclassical model may induce erratic dynamics in the capital-labor ratio under strong nonlinearity presented by the larger value

of  $\theta$ . There is a sharp difference between dynamics generated by the continuous and discrete models. To discuss emergence of irregular fluctuations in the continuous model, it may be helpful to take account two facts; one is that a simple nonlinear delay differential equation such as the Mackey-Glass equation (1977) may display complex dynamics involving chaos and the other is that there is always a time delay due to the decision making process and the decision implementation. In this and next sections, we will confine our attention to delays in the capital accumulation process. Using the mound-shaped production function as, for example, in the case of the modified production function (12), we take a close look at destabilizing effects caused by delays in production.

If a production delay is present and the delay is known or certain, then the production function is written as

$$y(t) = f(k(t - \tau))$$

where  $\tau \geq 0$  is the delay. We will examine the case of known delays in the next section and inquire into the case of unknown delay in this section. A convenient way to introduce unknown or uncertain delay into the model is offered by considering it as a random variable and replacing it by its expected value. If the expected per-capita capital stock at time  $t$  is denoted by  $k^e(t)$  and is based on the entire history of the actual capital stock from zero to  $t$ , then the continuous-time dynamic system (7) with delay in production can be rewritten as a Volterra-type integro-differential equation:

$$\begin{aligned} \dot{k}(t) &= -\alpha k(t) + \beta k^e(t)(1 - k^e(t)), \\ k^e(t) &= \int_0^t \omega(t - \sigma, T, m) k(\sigma) d\sigma, \end{aligned} \tag{14}$$

where  $\alpha = \delta$ ,  $\beta = sA$  and the weighting function is defined as

$$\omega(t - \sigma, T, m) = \begin{cases} \frac{1}{T} e^{-\frac{t-\sigma}{T}} & \text{if } m = 0, \\ \frac{1}{m!} \left(\frac{m}{T}\right)^{m+1} (t - \sigma)^m e^{-\frac{m(t-\sigma)}{T}} & \text{if } m \geq 1 \end{cases} \tag{15}$$

with  $\tau = t - \sigma$ . Here the shape parameter  $m$  is a nonnegative integer and  $T$  is a positive constant, which is associated with the length of the delay. If  $m = 0$ , then weights are exponentially decreasing with the largest weight given to the most current data. If  $m \geq 1$ , then the weighting function has a bell-shaped curve implying that the most current data has zero weight, the weight increases to a maximal value at  $t - \sigma = T$  and decreases thereafter. A steady state of (14) is obtained by setting  $\dot{k}(t) = 0$  and  $k(t) = k^e(t) = k^*$ ,

$$k^* = \frac{\beta - \alpha}{\beta} < 1.$$

To ensure positivity of the steady state, we make the following assumption:

**Assumption 2.**  $\beta - \alpha > 0$ .

To examine local dynamics of the above system in the neighborhood of the steady state, we consider its linearized version. The approximated nonlinear term evaluated at the steady state is

$$\begin{aligned}\beta \frac{d}{dk^e} k^e(t)(1 - k^e(t)) &= \beta(1 - 2k^*)k_\delta(t) \\ &= (2\alpha - \beta)k_\delta(t),\end{aligned}$$

where  $k_\delta = k - k^*$  denotes deviation from the steady state. The linearization yields

$$\dot{k}_\delta(t) = -\alpha k_\delta(t) + (2\alpha - \beta) \int_0^t w(t - \sigma, T, m) k_\delta(\sigma) d\sigma. \quad (16)$$

At the steady state, we look for the solution in the usual exponential form

$$k_\delta(t) = e^{\lambda t} u$$

which is substituted into the linearized equation (16)

$$\lambda e^{\lambda t} u = -\alpha e^{\lambda t} u + (2\alpha - \beta) \int_0^t w(t - \sigma, T, m) e^{\lambda \sigma} u d\sigma.$$

Notice that  $\tau = t - \sigma$ , then

$$\begin{aligned}\int_0^t w(t - \sigma, T, m) e^{\lambda \sigma} d\sigma &= \int_t^0 w(\tau, T, m) e^{\lambda(t-\tau)} (-d\tau) \\ &= e^{\lambda t} \int_0^t w(\tau, T, m) e^{-\lambda \tau} d\tau\end{aligned}$$

By letting  $t \rightarrow \infty$ , the integral part converges to

$$\int_0^\infty w(\tau, T, m) e^{-\lambda \tau} d\tau = \left(1 + \frac{\lambda T}{q}\right)^{-(m+1)}$$

with

$$q = \begin{cases} 1 & \text{if } m = 0, \\ m & \text{if } m \geq 1. \end{cases}$$

Substituting this expression into the integral part of the linearized equation, dividing both sides of the resultant expression by  $e^{\lambda t} u$  and arranging terms, we obtain the characteristic equation

$$-(2\alpha - \beta) + (\alpha + \lambda) \left(1 + \frac{\lambda T}{q}\right)^{m+1} = 0. \quad (17)$$

It has been already shown that the continuous-time neoclassical model without time delay is locally stable. By continuity, it can be supposed that the delay model is locally stable if the delay is small enough. We start our examination with a general result which generates local asymptotical stability regardless of the size of the delay and the shape of the weighting function.

**Theorem 1** *The steady state  $k^*$  of the distributed delay differential equation (14) is locally asymptotically stable if  $|2\alpha - \beta| \leq \alpha$ , regardless of the values of  $m$  and  $T$ .*

**Proof.** Notice first that  $\lambda = 0$  is not an eigenvalue under Assumption 2. Assume that  $\lambda \neq 0$  and  $\text{Re } \lambda \geq 0$ . Then

$$|\lambda + \alpha| > \alpha \text{ and } \left| 1 + \frac{\lambda T}{q} \right| > 1$$

implying that

$$\left| (\alpha + \lambda) \left( 1 + \frac{\lambda T}{q} \right)^{m+1} \right| > \alpha.$$

This relation and condition  $|2\alpha - \beta| \leq \alpha$  imply that the two terms in the left hand side of the characteristic equation (17) have different absolute values, thus  $\lambda \neq 0$  with  $\text{Re } \lambda \geq 0$  cannot be an eigenvalue. ■

Theorem 1 implies that the time delay is harmless to stability if  $\beta \leq 3\alpha$ . In order to examine a possibility of stability loss, we make the following assumption, which makes Assumption 2 redundant:

**Assumption 3.**  $\beta > 3\alpha$ .

The characteristic equation (17) is a polynomial equation with degree  $n = m + 2$  having the form

$$a_0 \lambda^n + a_1 \lambda^{n-1} + \dots + a_{n-1} \lambda + a_n = 0$$

with all real coefficients. Suppose that  $a_0$  is positive. Then the Routh-Hurwitz theorem states that necessary and sufficient conditions for all roots of this polynomial equation to have negative real parts are given by

(1) all coefficients are positive,  $a_k > 0$  for  $k = 0, 1, 2, \dots, n$ ,

(2)  $\Delta_1 > 0, \Delta_2 > 0, \dots, \Delta_n > 0$ ,

where  $\Delta_1, \Delta_2, \dots, \Delta_n$  are the leading principal minors of the Routh-Hurwitz matrix

$$\begin{bmatrix} a_1 & a_3 & a_5 & a_7 & \dots & 0 \\ a_0 & a_2 & a_4 & a_6 & \dots & 0 \\ 0 & a_1 & a_3 & a_5 & \dots & 0 \\ 0 & a_0 & a_2 & a_4 & \dots & 0 \\ 0 & 0 & a_1 & a_3 & \dots & 0 \\ \dots & \dots & \dots & \dots & \dots & \dots \\ 0 & 0 & 0 & 0 & \dots & a_n \end{bmatrix}.$$

Since general stability results cannot be obtained analytically, we will specify the values of parameters and consider special cases.

**Case 1**  $T = 0$ .

$T = 0$  corresponds to the model without delay. Taking  $T = 0$  in the characteristic equation gives the unique characteristic root,

$$\lambda = \alpha - \beta$$

which is negative under Assumption 3. Local stability under the general form of the production function satisfying Assumption 1 is already shown in (8). Here we have local asymptotic stability under the specific production function (12) without time delay. This result implies that a strong nonlinearity alone cannot be a source of complex dynamics in the continuous-time model. This shows a sharp contrast to dynamic results in nonlinear discrete-time models, in which a strong nonlinearity itself is a source of complex dynamics.

**Case 2**  $T > 0$  and  $m = 0$ .

By substituting  $m = 0$  and  $q = 1$  into (17), we obtain the quadratic characteristic equation

$$T\lambda^2 + (1 + \alpha T)\lambda + \beta - \alpha = 0. \quad (18)$$

Since  $a_0 = T > 0$ ,  $a_1 = 1 + \alpha T > 0$  and  $a_2 = \beta - \alpha > 0$ , then  $\Delta_1 > 0$  and  $\Delta_2 = a_1 a_2 > 0$ . Due to the Routh-Hurwitz criterion, we have local asymptotic stability when the weighting function is exponentially declining.

**Case 3**  $T > 0$  and  $m = 1$ .

In this case, the characteristic equation becomes cubic in  $\lambda$ ,

$$T^2\lambda^3 + T(2 + \alpha T)\lambda + (1 + 2\alpha T)\lambda + \beta - \alpha = 0. \quad (19)$$

All coefficients are positive,  $a_0 = T^2 > 0$ ,  $a_1 = T(2 + \alpha T) > 0$ ,  $a_2 = (1 + 2\alpha T) > 0$  and  $a_3 = \beta - \alpha > 0$ . Then the stability condition is that the leading principle minors are positive,

$$\Delta_1 = a_1 > 0,$$

$$\Delta_2 = a_1 a_2 - a_0 a_3 > 0,$$

$$\Delta_3 = a_3(a_1 a_2 - a_0 a_3) > 0.$$

The first and third inequalities are satisfied, given the second. We, therefore, have asymptotical stability if and only if  $\Delta_2 > 0$ , that is,

$$\begin{aligned} a_1 a_2 - a_0 a_3 &= T(2 + \alpha T)(1 + 2\alpha T) - T^2(\beta - \alpha) \\ &= T \{2\alpha^2 T^2 + (6\alpha - \beta)T + 2\} > 0. \end{aligned}$$

Let us denote the expression in the parentheses by  $\varphi(T)$ . It is quadratic in  $T$  and its discriminant is

$$D = (\beta - 2\alpha)(\beta - 10\alpha).$$

Under Assumption 3, the first factor is positive, so we can identify the following three cases.

(i) If  $3\alpha < \beta < 10\alpha$ , then  $D < 0$  indicating that  $\varphi(T)$  has no real roots. Consequently  $\Delta_2 = T\varphi(T) > 0$  holds for all  $T > 0$ , implying asymptotic stability of the steady state.

(ii) If  $\beta = 10\alpha$ , then  $D = 0$  so  $\varphi(T)$  has only one root (with multiplicity two)

$$T^* = -\frac{6\alpha - \beta}{4\alpha^2} = \frac{1}{\alpha} > 0.$$

Thus  $\Delta_2 > 0$  holds for all  $T \neq T^*$ , implying asymptotic stability for all  $T$  except a configuration of  $(\alpha, \beta, T)$  such that  $\alpha T = 1$  and  $\beta = 10\alpha$ .

(iii) If  $\beta > 10\alpha$ , then  $D > 0$  indicating that  $\varphi(T)$  has two real roots,  $T_1^*$  and  $T_2^*$  such as  $0 < T_1^* < T_2^*$  where

$$T_{1,2}^* = \frac{\beta - 6\alpha \pm \sqrt{(\beta - 2\alpha)(\beta - 10\alpha)}}{4\alpha^2}.$$

It is clear that  $\Delta_2 > 0$  holds for  $T < T_1^*$  or  $T > T_2^*$  and  $\Delta_2 < 0$  for  $T_1^* < T < T_2^*$ . Therefore we have asymptotic stability if  $T < T_1^*$  or  $T > T_2^*$  and local instability if  $T_1^* < T < T_2^*$ . So stability is lost at  $T = T_1^*$  and is regained at  $T = T_2^*$ . Notice that  $(\alpha T_1^*)(\alpha T_2^*) = 1$ .

We visualize the analytical results obtained above in Figure 1. Given a value of  $\alpha$ , the whole region of  $(\beta, T)$  is divided into two parts by the partition curve,  $\Delta_2 = 0$ ; the gray region is the instability region with  $\Delta_2 < 0$  and the white region is the stability region with  $\Delta_2 > 0$ . The red point on the  $\Delta_2 = 0$  curve implies that the characteristic roots are multiple for  $\beta = 10\alpha$  and  $T = 1/\alpha$ . From the above analysis, we can draw the following conclusion in the case of  $m = 1$ . If  $\beta < 10\alpha$ , then the stationary point is locally asymptotically stable regardless of the value of  $T$ . Returning to the definitions, the value of  $\alpha = n + s\mu$  depends on model parameter values and  $\beta = sA$  is the product of the marginal propensity to save and the technology parameter. Since we need a large value of the technology parameter to reverse this inequality, the high technological progress may be a source of instability. Assume next that  $\beta > 10\alpha$ . The delay has to be sufficiently small or sufficiently large to guarantee local asymptotical stability. For example, when  $\beta = 12\alpha$ , the threshold values of  $T$  are

$$T_1^* = \frac{3 - \sqrt{5}}{2\alpha} < \frac{1}{\alpha} \text{ and } T_2^* = \frac{3 + \sqrt{5}}{2\alpha} > \frac{1}{\alpha},$$

both of which are indicated by the two black points on the separation curve  $\Delta_2 = 0$  in Figure 1. The stationary point is locally unstable for  $T$  in the shaded region (i.e.,  $T_1^* < T < T_2^*$ ) and stable for  $T$  in the white region (i.e.,  $T < T_1^*$  or

$T > T_2^*$ ).

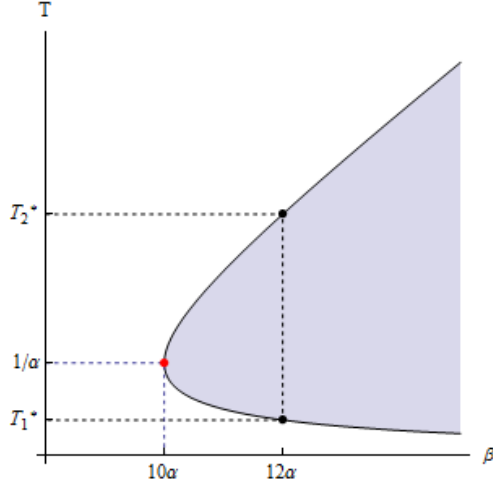


Figure 1. Stability and instability regions when  $m = 1$

We now return to the characteristic equation (19) and show the possibility of the birth of a limit cycle at the threshold values  $T = T_1^*$  and  $T = T_2^*$  by applying the Hopf bifurcation theorem. According to the theorem, we can establish the existence of a cyclic solution if the cubic characteristic equation has a pair of pure imaginary roots and the real parts of these roots change signs with a bifurcation parameter. At the critical values where  $\Delta_2 = 0$  or  $a_3 = a_1 a_2 / a_0$ , the characteristic equation can be rewritten as

$$a_0 \lambda^3 + a_1 \lambda^2 + a_2 \lambda + \frac{a_1 a_2}{a_0} = 0,$$

which factors as

$$\left( \lambda + \frac{a_1}{a_0} \right) (a_0 \lambda^2 + a_2) = 0$$

showing that one of the characteristic roots is real and negative,

$$\lambda_1 = -\frac{a_1}{a_0} = -\frac{2 + \alpha T}{T} < 0$$

and the other two are pure imaginary,

$$\lambda_{2,3} = \pm i \sqrt{\frac{a_2}{a_0}} = \pm i \sqrt{\frac{1 + 2\alpha T}{T^2}} = \pm i \gamma. \quad (20)$$

In order to apply the Hopf bifurcation theorem, we need to check whether the real part of the conjugate complex root changes its sign as the bifurcation parameter passes through its critical value. Selecting  $T$  as the bifurcation parameter, assuming  $\lambda = \lambda(T)$  and then differentiating the characteristic equation with respect to  $T$ , we obtain, after arranging terms, the derivative of  $\lambda(T)$ ,

$$\frac{d\lambda}{dT} = -\frac{2(T\lambda^3 + (1 + \alpha T)\lambda^2 + \alpha\lambda)}{3T^2\lambda^2 + 2(2T + \alpha T^2)\lambda + (1 + 2\alpha T)}.$$

Using the facts that the terms with  $\lambda$  are pure imaginary and the constant terms are real gives

$$\begin{aligned} \left[ \frac{d(\operatorname{Re} \lambda)}{dT} \right]_{\lambda=\pm i\gamma} &= \operatorname{Re} \left[ -\frac{2(T\lambda^3 + (1 + \alpha T)\lambda^2 + \alpha\lambda)}{3T^2\lambda^2 + 2(2T + \alpha T^2)\lambda + (1 + 2\alpha T)} \right]_{\lambda=\pm i\gamma} \\ &= \frac{2(1 + T_i^{*2}\gamma^2)}{(1 + 2\alpha T_i^* - 3T_i^{*2}\gamma^2)^2 + (4T_i^* + 2\alpha T_i^{*2})^2\gamma^2} (1 - \alpha T_i^*), \end{aligned}$$

where both the numerator and the denominator of the first factor are positive. Therefore we have

$$\left[ \frac{d(\operatorname{Re} \lambda)}{dT} \right]_{\lambda=\pm i\gamma} \geq 0 \text{ if } 1 \geq \alpha T_i^* \text{ for } i = 1, 2.$$

These inequalities imply that the roots cross the imaginary axis at  $i\gamma$  from left to right as  $T$  increases from  $T_1^* < 1/\alpha$  (i.e., stability is lost) and from right to left as  $T$  increases from  $T_2^* > 1/\alpha$  (stability is regained). In Figure 1, the stability loss occurs when  $T$  enters the gray unstable region from below and the stability regain occurs when  $T$  re-enters the white stable region from below.

In order to find what kind of dynamics is generated for  $T \in (T_1^*, T_2^*)$ , we perform numerical simulations. To this end, we transform the integro-differential dynamic system to the three-dimensional dynamic system of ordinary differential equations:

$$\begin{aligned} \dot{k}(t) &= -\alpha k(t) + \beta k^e(t) [1 - k^e(t)], \\ \dot{k}^e(t) &= \frac{1}{T} (x(t) - k^e(t)), \\ \dot{x}(t) &= \frac{1}{T} (k(t) - x(t)). \end{aligned}$$

The first equation is the same as the first equation of (14). With  $m = 1$ , the weighting function is

$$k^e(t) = \int_0^t \left( \frac{1}{T} \right)^2 (t - \sigma) e^{-\frac{t-\sigma}{T}} d\sigma,$$

and the second equation is obtained by differentiating both sides of the above equation with respect to  $t$  and introducing the new variable

$$x(t) = \int_0^t \frac{1}{T} e^{-\frac{t-\sigma}{T}} k^e(\sigma) d\sigma.$$

The third equation is obtained by differentiating  $x(t)$  with respect to  $t$ . Needless to say, the characteristic equation of this 3D system is identical with (19).

Returning to Figure 1, taking  $\beta = 12\alpha$  with  $\alpha = 1$  and increasing  $T$  from a little bit smaller value than  $T_1^*$  to a little bit larger value than  $T_2^*$  yield the bifurcation-like diagram as is presented in Figure 2(A). It is shown that the stationary point  $k^*$  is asymptotically stable for  $T < T_1^*$  and  $T > T_2^*$  and it bifurcates to cyclic behavior if  $T$  is between  $T_1^*$  and  $T_2^*$ . For each value of  $T$ , the dynamic 3D system is solved and we measure a time series of  $k(t)$ ,  $k^e(t)$

and  $x(t)$  for  $3000 \leq t \leq 4000$ . The extreme values (i.e., local maximums and local minimums) of the time series  $k(t)$  are plotted in blue over each  $T$ . The two (upper and lower) blue curves mean that a periodic cycle generated for each  $T \in (T_1^*, T_2^*)$  has one maximum and one minimum. In Figure 2(B) we take  $T_a = (T_1^* + T_2^*)/2$  and depict the periodic cycle in blue in the phase plane of  $k^e(t)$  and  $k(t)$ , which describes the dynamic flow based on the measured data. It can be seen that points  $k_H$  and  $k_L$  are the maximum and minimum values of the cycle when  $T = T_a$ . Two observations can be made: first, there are two points for each  $T \in (T_1^*, T_2^*)$  implying that the trajectories converge to a periodic cycle having one maximum and one minimum; second, some segments of the trajectories enter the negative region of  $k$ . One way to avoid such economically unfavorable phenomena that the capital dynamics might lead to negative quantities is to modify the capital dynamic equation in such a way that

$$\dot{k}(t) = -\alpha k(t) + \beta \text{Max}\{0, k^e(t)[1 - k^e(t)]\}.$$

The simulation results with this modified dynamic equation are obtained in the same way and are depicted as the red curves in Figure 2(A) in which the trajectories of capital stay in the positive region for  $T \in (T_1^*, T_2^*)$ . The red cycle in Figure 2(B) is in the first quadrant of the phase plane and has the maximum  $k_h$  and the minimum  $k_l$ . The point  $k_j$  for  $j = H, h, \ell, L$  in Figure 2(A) corresponds to the same point in Figure 2(B). We will return to the second observation in the final section.

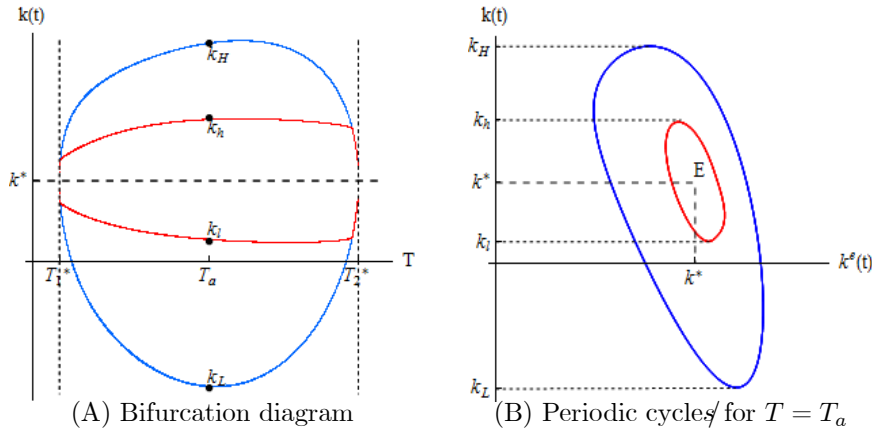


Figure 2. Birth of cyclic behavior when stability is lost

**Case 4**  $T > 0$  and  $m = 2$ .

Substituting  $m = 2$  into the characteristic equation (17) yields the following fourth-order equation

$$a_0\lambda^4 + a_1\lambda^3 + a_2\lambda^2 + a_3\lambda + a_4 = 0$$

where

$$a_0 = T^3 > 0, \quad a_1 = T^2(6 + \alpha T) > 0, \quad a_2 = 6T(2 + \alpha T) > 0,$$

$$a_3 = 4(2 + 3\alpha T) > 0 \text{ and } a_4 = 8(\beta - \alpha) > 0.$$

All coefficients are positive. In the case of a fourth-order equation, the basic Routh-Hurwitz matrix is

$$\begin{pmatrix} a_1 & a_3 & 0 & 0 \\ a_0 & a_2 & a_4 & 0 \\ 0 & a_1 & a_3 & 0 \\ 0 & a_0 & a_2 & a_4 \end{pmatrix}$$

with leading minors

$$\Delta_1 = a_1 > 0,$$

$$\Delta_2 = 2T^3(3T^2\alpha^2 + 18T\alpha + 32) > 0,$$

$$\Delta_3 = 8T^3 \{64 + 12T(14\alpha - 3\beta) + 12T^2\alpha(6\alpha - \beta) + T^3\alpha^2(10\alpha - \beta)\} \geq 0,$$

$$\Delta_4 = \Delta_3 a_4 > 0 \text{ provided that } \Delta_3 > 0.$$

Therefore  $\Delta_3 > 0$  suffices to achieve local asymptotic stability. Notice that  $\Delta_3 = 0$  if the cubic equation in  $T$  in the braces is equal to zero. The discriminant of this cubic equation is

$$\begin{aligned} D &= -4A_1^3A_3 + A_1^2A_2^2 - 4A_0A_2^3 + 18A_0A_1A_2A_3 - 27A_0^2A_3 \\ &= 442368\alpha^3(\beta - 2\alpha)^2(\beta - 6\alpha) \end{aligned}$$

where  $A_0 = 64$ ,  $A_1 = 12(14\alpha - 3\beta)$ ,  $A_2 = 12\alpha(6\alpha - \beta)$  and  $A_3 = \alpha^2(10\alpha - \beta)$ . The cubic equation  $\Delta_3 = 0$  can be reduced to  $4(-2 + \alpha T)^2(4 + \alpha T) = 0$  if  $\beta = 6\alpha$ . It is then clear that the cubic equation has the unique root with multiplicity two for  $\beta = 6\alpha$  and  $T = 2/\alpha$ . By taking the same procedure as in the case of  $m = 1$ , we can show that the dynamic system with  $m = 2$  generates cyclic behavior when the local stability is violated, as illustrated in Figure 3. It is possible to examine the case with  $m \geq 3$ . However, calculations becomes longer and more clumsy.

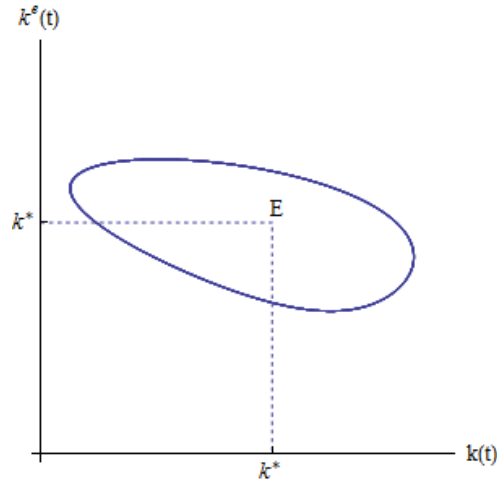


Figure 3. Birth of a limit cycle when  $m = 2$ ,  $\alpha = 1$ ,  $\beta = 7$  and  $T = 1$

## 4 Growth Model with Fixed Time Delay

A fixed time delay is an appropriate approach to deal with the case in which the delay is certain. If  $\tau$  represents the time delay inherent in the production process, then the per-capita production function reflecting the influence of pollutions is described by

$$f(k(t - \tau)) = Ak(t - \tau)((1 - k(t - \tau))).$$

By replacing  $k^e(1 - k^e)$  in the first equation of (14) by this expression, we obtain a fixed delay differential equation

$$\dot{k}(t) = -\alpha k(t) + \beta k(t - \tau)(1 - k(t - \tau)). \quad (21)$$

The dynamics of this equation is examined henceforth. A stationary point of the capital accumulation dynamics is obtained by solving  $\dot{k}(t) = 0$  with  $k(t) = k(t - \tau) = k$ . A simple calculation shows that it is identical with  $k^*$  obtained under the continuously distributed time delay.

Following the tradition of the study on fixed delay equations, we start from the local stability analysis of the stationary state and then consider the question of *stability switching* of the fixed delay equation (21). The stability of the stationary state depends on the location of the roots of the associated characteristic equation. The stability analysis concerns with whether all roots lie in the left half of the complex plane. The location of the roots, in turn, depends on the value of the delay. The stability switching analysis concerns with whether roots cross the imaginary axis when the delay changes.

For the first purpose, we make a linear approximation of the nonlinear delay equation (21) to obtain its variational equation,

$$\dot{k}_\delta(t) = -\alpha k_\delta(t) + \beta(1 - 2k^*)k_\delta(t - \tau)$$

where  $k_\delta(t) = k(t) - k^*$  is the deviation from the stationary state. This is a first-order delay differential equation of retarded type. We look for the solution in the usual exponential form  $k_\delta(t) = e^{\lambda t}u$ . Substituting this expression into the variational equation and noticing that  $\beta(1 - 2k^*) = 2\alpha - \beta$ , we have the corresponding characteristic equation,

$$(\lambda + \alpha) - (2\alpha - \beta)e^{-\lambda\tau} = 0. \quad (22)$$

Without time delay (i.e.,  $\tau = 0$ ), the characteristic root is  $\lambda = -(\beta - \alpha) < 0$ . Thus the steady state  $k^*$  is a stable fixed point which is attained for any non-zero initial point. We can also obtain the following stability result for the fixed delay model with  $\tau > 0$ , which corresponds to Theorem 1 obtained in the case of distributed-delay models:

**Theorem 2** *The steady state  $k^*$  of the fixed delay dynamic equation (21) is locally asymptotically stable if  $|2\alpha - \beta| \leq \alpha$ , regardless of the value of the fixed time delay  $\tau$ .*

**Proof.** Assume to the contrary that for an eigenvalue,  $\text{Re } \lambda \geq 0$ . Then

$$\begin{aligned} e^{-\lambda\tau} &= e^{-(\text{Re } \lambda)\tau} e^{-i(\text{Im } \lambda)\tau} \\ &= e^{-(\text{Re } \lambda)\tau} (\cos((\text{Im } \lambda)\tau) - i \sin((\text{Im } \lambda)\tau)). \end{aligned}$$

So  $|e^{-\lambda\tau}| = |e^{-(\operatorname{Re}\lambda)\tau}| \leq 1$ . Notice that since  $\lambda \neq 0$ ,

$$|\lambda + \alpha| > \alpha$$

and

$$|(2\alpha - \beta)e^{-\lambda\tau}| \leq |2\alpha - \beta|.$$

Under condition  $|2\alpha - \beta| \leq \alpha$ , the absolute values of the two terms of the characteristic equation are different and thus  $\lambda \neq 0$  with  $\operatorname{Re}\lambda \geq 0$  cannot be an eigenvalue. This completes the proof. ■

Theorem 2 ensures that the fixed time delay is harmless if  $\beta \leq 3\alpha$ . Even if this sufficient condition is violated, it can be supposed, due to continuity, that  $k^*$  can be still stable for a smaller value of  $\tau$ . It is also expected that as the length of the delay increases, stability of the stationary state may change (i.e., stability switch). In order to understand this phenomena, it is crucial to determine a threshold value of  $\tau$  for which the characteristic equation has a pair of conjugate pure imaginary roots. Since  $\lambda = 0$  is not a root of the characteristic equation, we can assume without loss of generality that  $\lambda = i\omega$  with  $\omega > 0$  is a root. Substituting it into the characteristic equation, we can write the real and imaginary parts as:

$$\begin{aligned} \alpha - (2\alpha - \beta)\cos\omega\tau &= 0, \\ \omega + (2\alpha - \beta)\sin\omega\tau &= 0. \end{aligned} \tag{23}$$

The sum of the squares of the two equations yields

$$\omega^2 = (\beta - \alpha)(\beta - 3\alpha)$$

implying that

$$\omega_+ = \sqrt{(\beta - \alpha)(\beta - 3\alpha)},$$

which is real and positive under Assumption 3. Solving the first equation of (23) for  $\tau$  and substituting  $\omega_+$  into the resultant expression yields the threshold value of time delay for which stability switching may occur

$$\tau^* = \frac{\cos^{-1}\left(\frac{\alpha}{2\alpha - \beta}\right)}{\sqrt{(\beta - \alpha)(\beta - 3\alpha)}} \equiv \phi(\beta, \alpha). \tag{24}$$

In order to observe stability switching, we need to determine the sign of the derivative of the real part of the purely imaginary root. We can select  $\tau$  as the bifurcation parameter and consider the characteristic equation as a continuous function in terms of the delay  $\tau$ . Differentiating the characteristic equation with respect to  $\tau$  yields

$$(1 + (2\alpha - \beta)\tau e^{-\lambda\tau}) \frac{d\lambda}{d\tau} = -(2\alpha - \beta)\lambda e^{-\lambda\tau}.$$

For convenience, we study  $(d\lambda/d\tau)^{-1}$  instead of  $d\lambda/d\tau$ . Then we have

$$\left(\frac{d\lambda}{d\tau}\right)^{-1} = \frac{1 + (2\alpha - \beta)e^{-\lambda\tau}\tau}{-\lambda(2\alpha - \beta)e^{-\lambda\tau}}$$

and from the characteristic equation we obtain

$$e^{-\lambda\tau} = \frac{\lambda + \alpha}{2\alpha - \beta}.$$

Thus

$$\begin{aligned} \left[ \operatorname{Re} \left( \frac{d\lambda}{d\tau} \right)^{-1} \right]_{\lambda=i\omega} &= \operatorname{Re} \left( \frac{e^{\lambda\tau}}{-\lambda(2\alpha - \beta)} - \frac{\tau}{\lambda} \right)_{\lambda=i\omega} \\ &= \operatorname{Re} \left( -\frac{1 + \tau(\lambda + \alpha)}{\lambda(\lambda + \alpha)} \right)_{\lambda=i\omega} \\ &= \operatorname{Re} \left( \frac{\omega^2(1 + \tau\alpha) - \tau\omega^2\alpha}{\omega^4 + \omega^2\alpha^2} \right) \\ &= \frac{1}{\omega^2 + \alpha^2} > 0. \end{aligned}$$

The last inequality implies that the crossing of the imaginary axis is from the left to the right as  $\tau$  increases and thus results in the loss of stability. In other words, the fixed delay has a destabilizing effect since the real part turns to be positive from negative as the delay becomes longer. In summary we have the following:

**Theorem 3** *Under Assumption 3, the neoclassical growth model with fixed time delay is locally asymptotically stable when  $\tau < \tau^*$  and unstable when  $\tau > \tau^*$  where the critical level of time delay  $\tau^*$  is defined by*

$$\tau^* = \frac{\cos^{-1} \left( \frac{\alpha}{2\alpha - \beta} \right)}{\sqrt{(\beta - \alpha)(\beta - 3\alpha)}}.$$

Locally stable and unstable combinations of  $\beta$  and  $\tau$  are graphed in Figure 4 where  $\alpha$  is taken to be 1. The dotted vertical locus,  $\beta = 3\alpha$ , divides the whole  $(\beta, \tau)$  region into two parts; the steady state  $k^*$  is definitely locally stable in the left of the locus due to Theorem 2. Further, the black-bold locus of  $\tau^* = \phi(\beta, \alpha)$  is asymptotic to the  $\beta = 3\alpha$  locus and the horizontal axis and divides the remaining region into two parts: the steady state is locally stable for  $(\beta, \tau)$  in the region below this locus and unstable above. Since this partition curve between the stable and unstable regions is downward-sloping, larger (respectively smaller) values of the two variables contribute instability (respectively stability) while a trade-off between the two is necessary to preserve stability. We now turn attention to the instability region above the partition curve. It is colored and shows a bifurcation diagram with respect to  $\beta$  and  $\tau$ . Different colors indicate different periods of cycles up to 16. Periodic cycle with a period larger than 16 and aperiodic cycle are colored in red. A period of one cycle is defined by a number of crossing of a time-trajectory with the  $k = k^*$  locus from above within one cycle (from one peak to the next peak or from one trough to the next trough). This diagram shows that the delay dynamic equation (21) generates a wide variety of dynamics ranging from a simple limit cycle to chaotic fluctuations when stability is lost. As is seen shortly, the dynamic equation gives rise a period-one cycle for a combination of  $\beta$  and  $\tau$  in the purple region

just above the separation curve, a period-two cycle for a combination in the dark purple region above the purple region, a period-four cycle in the thin blue region and chaos in the red region. The equilibrium point goes to chaos via the period-doubling cascade that displays a sequence of bifurcations in which the period of the cycle doubles as a parameter combination is changed slightly.

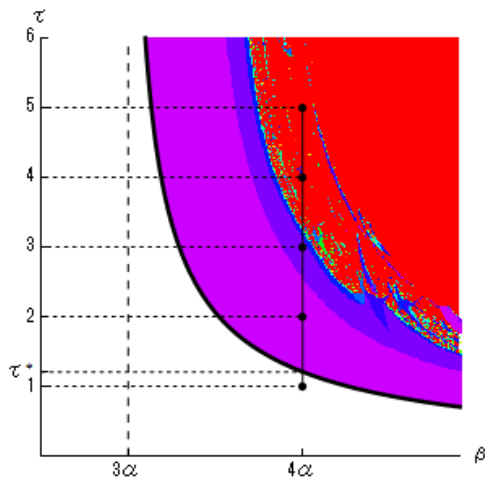


Figure 4. Two-parameter bifurcation diagram of the fixed delay equation (21)

To check what dynamics emerges in each different colored region, we take  $\alpha = 1$ ,  $\beta = 4\alpha$ , pick up three dotted points,  $(4\alpha, 2)$ ,  $(4\alpha, 3)$  and  $(4\alpha, 4)$  along the vertical real line in Figure 4 and then perform simulations under these specifications of the bifurcation parameters. These show a sequence of a time trajectory and  $(k(t), k(t - \tau))$  plots of these time delay embeddings for three different values of  $\tau$ . Notice that  $k(t - \tau)$  is the ordinate in both diagrams in each part of Figure 5 to make comparison easier. When  $\tau = 2$ , as shown in Figure 5(A), a time trajectory regularly repeats ups and downs and intersects the  $k = k^*$  locus once from above within one cycle. That is, the plot of  $k(t)$  and  $k(t - \tau)$  forms a simple limit cycle which we call a period-one cycle. The dynamic system with any parametric combination in the purple region exhibits the same dynamics. When  $\tau$  is increased to 3, then Figure 5(B) shows that regularity of the time trajectory is distorted and there are three local maxima and three local minima within one cycle. However it is also observed that the time-trajectory intersects the  $k = k^*$  locus twice from above implying that a period-two cycle was born as depicted in the  $(k(t), k(t - \tau))$  plane. When  $\tau = 4$ , as shown in Figure 5(C), the time trajectory exhibits erratic fluctuations implying a very long period or chaos. Accordingly the return map also displays chaotic motions. Although it is not presented here, we have numerically confirmed that the dynamics with parameters in the red region have initial point dependency so that arbitrarily

close two initial conditions diverge as time proceeds.

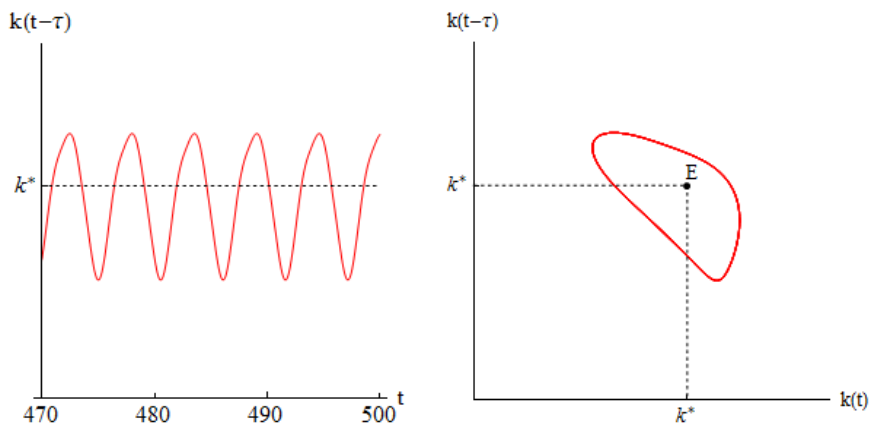


Figure 5(A). Periodic cycle with  $\tau = 2$

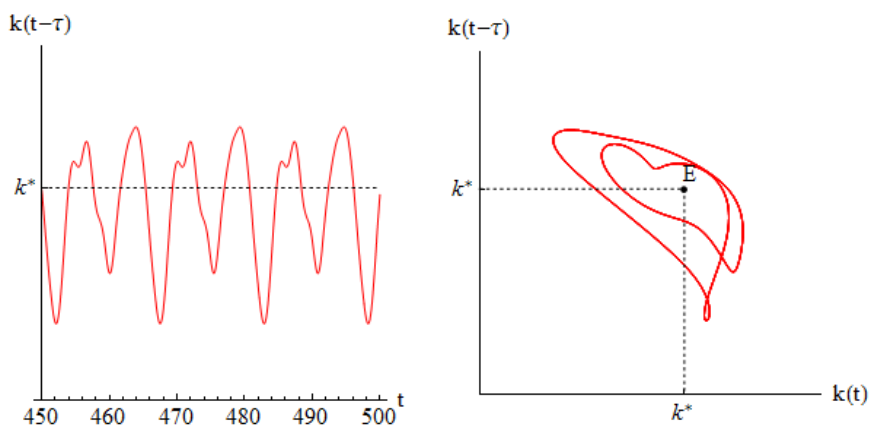


Figure 5(B). Periodic cycle with  $\tau = 3$

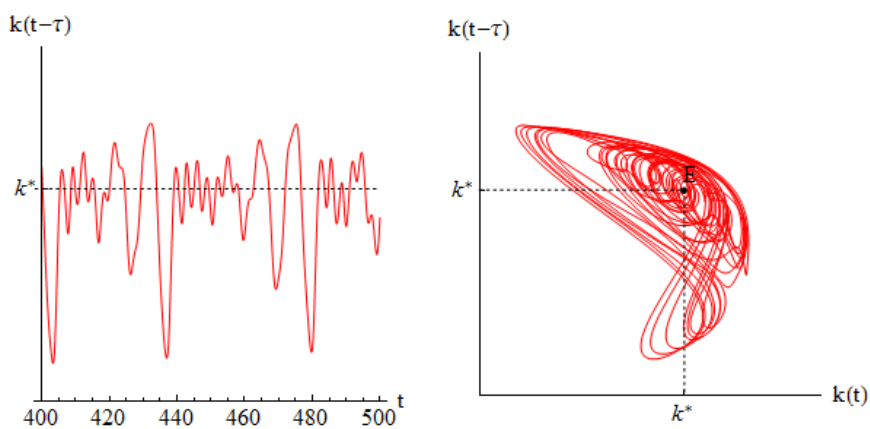


Figure 5(C) Aperiodic cycle with  $\tau = 4$

To extend the above analysis, we continuously increase the value of  $\tau$  from 1 to 5 along the vertical real line in Figure 4. When the value of  $\tau$  passes the threshold value  $\tau^* = \phi(\beta, \alpha)$ , which is approximately 1.29 for the specified values of  $\alpha$  and  $\beta$ , the fixed point loses its stability and bifurcates to a periodic solution. Simulation results are summarized in a bifurcation-like diagram of  $k(t)$  against  $\tau$  in Figure 6. It is constructed in the following way. For each value of  $\tau > \tau^*$ , the delay equation (21) is numerically solved for  $0 < t \leq 400$ , given an initial function  $\varphi(t) = 0.5$  for  $t \in [-\tau, 0]$ . The local maximums and minimums of the time trajectory for  $t \in [300, 400]$  are plotted above the selected value of  $\tau$ . This diagram exhibits a number of local maximum and local minimum within one cycle so it is more likely to the Poincare section. As is already seen above, a time-trajectory has one local maximum and one local minimum for  $\tau = 2$  so that there are two points over  $\tau = 2$ . Two points bifurcates to four extrema that turn to six extrema, shortly after two more points come in. We have already checked that the period-two cycle has six extrema when  $\tau = 3$  as shown in Figure 6 where the vertical dotted line at  $\tau = 3$  crosses six time the red colored graphs. Although the bifurcation of the extremes does not follow exactly period-doubling, this process repeats itself to generate periodic cycles with higher periods and then chaotic fluctuations.

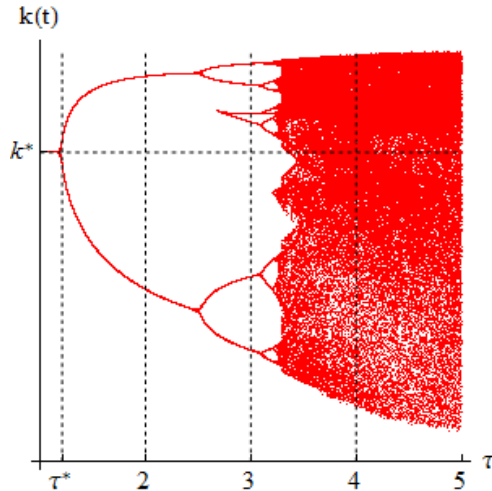


Figure 6. Bifurcation diagram with respect to  $\tau$ , given  $\alpha = 1$  and  $\beta = 4\alpha$

## 5 Comparison of Continuously Distributed and Fixed Delays

No matter which time delay is introduced into the neoclassical growth model, it is found that the delay has a destabilizing effect if Assumption 3 is violated. In this section, we compare the destabilizing effect caused by the continuously distributed time delay with the one by the fixed time delay. We have obtained the instability and stability regions separated by equation (24) under the fixed time delay. We have also obtained the stability regions divided by  $\Delta_2 = 0$  when  $m = 1$  and  $\Delta_3 = 0$  when  $m = 2$  under continuously distributed time delay. Repeating the same procedure for  $m = 3$  through 5, we get three more partition curves that divide the  $(\beta, T)$  space into the stable and unstable regions. The

specified forms of these separation curves, however, are not given here because of their too-long expressions. Then given  $\alpha = 1$ , the  $\tau^* = \phi(\beta, \alpha)$  curve colored in red and the five black partition curves with  $m$  from 1 to 5 are illustrated in Figure 7. The four red points there correspond to the combination of  $(\beta, T)$  for which the partition equations have multiple roots, although it is not easy to recognize that all these separation curves have fork-shaped profiles. It can be seen that all of the partition curves with continuously distributed time delay are located in the gray region where the steady state is locally unstable under the fixed time delay and approaching the partition curve with fixed time delay from the right as the value of  $m$  increases.

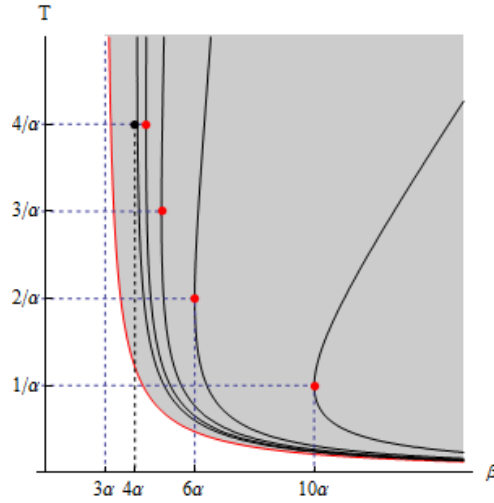


Figure 7. Partition curves of continuously distributed and fixed time delays

It is natural to guess that the distributed stable region becomes gradually smaller and converges to the fixed stable region when  $m$  tends to infinity. This is confirmed to be correct if we notice the properties of the weighting function. For  $m \geq 1$ , it takes a bell-shaped profile. As  $m$  increases, the function becomes more peaked around  $t - \sigma$  and tends to the Dirac delta function. For sufficient large  $m$ , the weighting function may be regarded as very close to the Dirac delta function and the dynamic behavior under the continuously distributed time delay is very similar to the one under the fixed time delay. We can explain this phenomenon mathematically. Given  $m \geq 1$ , the characteristic equation (17) under continuously distributed time delay can be written as

$$\lambda + \alpha - \frac{2\alpha - \beta}{\left(1 + \frac{T}{m}\lambda\right)^m \left(1 + \frac{T}{m}\lambda\right)} = 0.$$

As  $m \rightarrow \infty$ , it converges to

$$\lambda + \alpha - (2\alpha - \beta)e^{-T\lambda} = 0$$

which is the characteristic equation (22) of the fixed time delay if  $T$  is replaced with  $\tau$ . In short, under continuously distributed time delay, although we comprehensively use the delayed or past data of capital, the stability region is sensitive to the shape of the weighting function. Increasing the value of  $m$

strengthens the destabilizing effect caused by the distributed delay in a sense that the stability region becomes smaller. It then converges to the fixed delay stability region as  $m \rightarrow \infty$ .

We now turn our attention to similarity and dissimilarity of dynamics generated under the fixed time delay to those generated under the continuously distributed time delay. To this end, we set  $\alpha = 1$ ,  $\beta = 4$  and  $\tau = 4$  which corresponds to the black point in Figure 7 and Figure 4. Given this configuration of the parameters, complex dynamics under the fixed time delay is obtained as illustrated in Figure 6 in which many points remain on the vertical dotted line  $\tau = 4$  or in Figure 5(C) in which the same dynamics is plotted in the  $(k(t), k(t - \tau))$  plane and seems to be very high-order cyclic or aperiodic. In order to see what dynamics the distributed model can generate under the same parametric condition, we reduce the integro-differential equation (14) to a system of ordinary differential equations. Since the equivalence is already shown in the case of  $m = 1$ , we assume that  $m > 1$ . The expected value of capital is given by

$$k^e(t) = \int_0^t \frac{1}{m!} \left(\frac{m}{T}\right)^{m+1} (t - \sigma)^m e^{-\frac{m(t-\sigma)}{T}} k(\sigma) d\sigma$$

and for all  $\ell = 0, 1, \dots, m$ , introduce the functions

$$x_\ell(t) = \int_0^t \frac{1}{\ell!} \left(\frac{m}{T}\right)^{\ell+1} (t - \sigma)^\ell e^{-\frac{m(t-\sigma)}{T}} k(\sigma) d\sigma$$

where  $x_m(t) = k^e(t)$ . Then by differentiation,

$$\dot{k}^e(t) = \frac{m}{T} (x_{m-1}(t) - k^e(t)) \text{ for } \ell = m,$$

$$\dot{x}_\ell(t) = \frac{m}{T} (x_{\ell-1}(t) - x_\ell(t)) \text{ for } \ell = 1, \dots, m - 1$$

and

$$\dot{x}_0(t) = \frac{m}{T} (k(t) - x_0(t)) \text{ for } \ell = 0.$$

Combining these  $m + 1$  equations with

$$\dot{k}(t) = -\alpha k(t) + \beta k^e(t)(1 - k^e(t))$$

yields the  $m + 2$  dimensional system of ordinary differential equations for  $k(t)$ ,  $k^e(t)$  and  $x_\ell(t)$ ,  $\ell = 0, 1, \dots, m - 1$ . Specifying the value of  $m$ , we perform simulations. When  $m = 10$ , the ODE system exhibits a periodic cycle with two extremes as shown in Figure 8(A). When  $m$  increases to 30, a periodic cycle with six extremes appears, as shown in Figure 8(B). When  $m$  becomes more than 50, erratic behavior may occur and the aperiodic behavior with  $m = 100$  is represented in Figure 8(C).

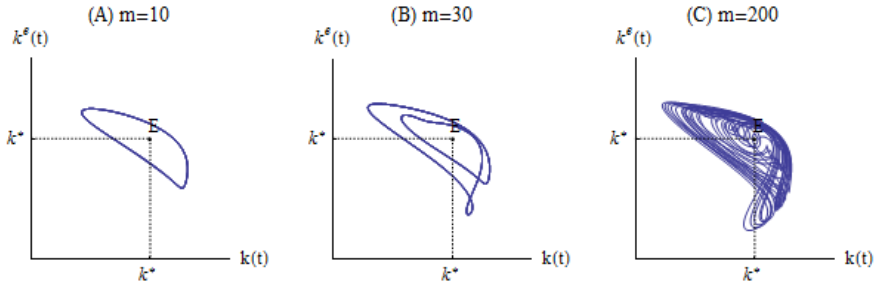


Figure 8. Return maps under continuously distributed time delay

Although Figures 8(A), (B) and (C) look similar to Figures 5 (A), (B) and (C), there is a distinctive difference: the values of  $\alpha$ ,  $\beta$  and  $\tau$  are fixed and  $m$  is altered in Figure 8 while the value of  $\alpha$  and  $\beta$  are fixed and  $\tau$  is changed in Figure 5. Notice however the similarity between Figure 5(C) and Figure 8(C), both are obtained under the same values of the parameters  $\alpha$ ,  $\beta$  and  $\tau$  and  $m = 200$ . So the following result is confirmed in a different way: the distributed delay model with high value of  $m$  generates similar dynamics as the fixed delay model. To measure the complexity of these dynamics generated by the ODE system, we calculate the maximum Lyapunov exponent against various values of  $m$  and the results are plotted in Figure 9 where ML on the ordinate stands for Maximum Lyapunov:

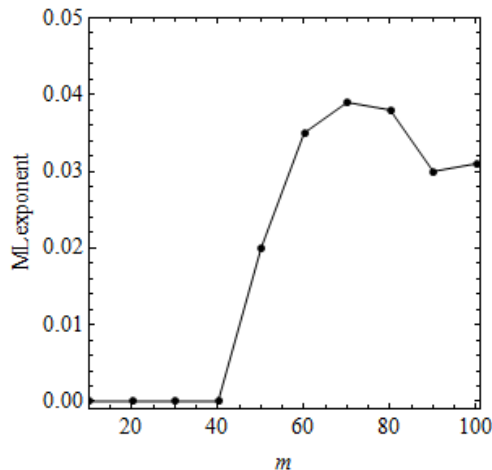


Figure 9 Maximum Lyapunov exponent againsts  $m$

The ODE system has zero maximum Lyapunov exponent for  $m$  below 40 and a positive maximum Lyapunov exponent for  $m$  greater than 50. That is, chaotic dynamics are born for some values of  $m$  between 40 and 50. The fixed delay model (14) can give rise to chaos as numerically confirmed in Figure 6. It looks like a simple equation, however, it is actually infinite dimensional dynamic system. If the distributed delay model with higher value of  $m$  can approximate dynamics generated by the fixed delay model, it can be safe to say that chaos generated by the fixed delay model is thought to be high dimensional chaos

since the distributed delay model can generate the similar complex dynamics only when  $m$  takes a large value. With these simulations and the results obtained in Section 3, we summarize the main points of the dynamic model with continuously distributed time delay:

**Theorem 4** *Under Assumption 3, dynamics in the neoclassical growth model with continuously distributed time delay is the following: (1) it is locally asymptotically stable when the shape parameter  $m$  is zero or unity; (2) it generate periodic cycles for  $2 \leq m \leq 40$ ; (3) it gives rise to aperiodic fluctuations for  $m \geq 50$ ; (4) it converges to the neoclassical growth model with fixed time delay as  $m$  goes to infinity.*

## 6 Concluding Remarks

The neoclassical growth model is developed in this paper with continuous time scales and two kinds of time delay. It complements the pioneering work of Day (1982) in which discrete-time and a production lag are assumed. Special function form is introduced to consider pollution in production, which results in the dynamic model equivalent to that induced by the logistic map. Our continuous-time model is similar in spirit and functional form to Day's discrete-time model.

The capital accumulation process has been formulated in a way that allows for both continuously distributed and fixed time delays. They are a clear consequence of delays in information gathering in the production process and in investment decisions. We start with the continuous model without time delay and confirm the well-known result that the steady state  $k^*$  is always asymptotically stable if  $\alpha < \beta$ . Our first concern of this paper is on the stability preservation in the delay models. Theorems 1 and 2 show that the same state  $k^*$  in the delay model is always asymptotically stable, regardless of the length of the time delay, if  $\beta \leq 3\alpha$ . This condition holds if the technology parameter  $A$  is sufficiently small. In addition to this, Case 2 with  $T > 0$  and  $m = 0$  implies asymptotic stability of  $k^*$ . Thus, our first conclusion is that the delay becomes harmless to stability of the steady state if the technology parameter takes a small value or the weighting function is exponentially declining.

Our second concern turns to the destabilizing effect caused by time delay when  $\beta > 3\alpha$ . In the case of continuously distributed time delay, the capital accumulation process becomes a set of integro-differential equations and under specified conditions, local instability may occur. The possibility of the birth of limit cycles is analytically verified based on Hopf bifurcation. The shape of the separation curves depends on the value of the shape parameter  $m$  of the weighting function. The separation curve takes a fork-shaped profile for a small number of  $m$  indicating that the time lag has to be sufficiently small or sufficiently large to guarantee local asymptotical stability as depicted in Figures 1 and 4. Further, numerical simulations show that some segments of the cyclic trajectories enter into the non-feasible negative region (Figure 2). This cannot happen if deviations of time delay from its critical values are small enough as shown in Figure 1 and Figure 3. However this is not the case in large deviations. In order to force the trajectory to move back to the positive region from zero values, we impose the non-negativity constraint on output in the capital dynamic

equation. This is a simple way to prevent trajectories from being negative. In a more sophisticated way, the mound-shaped production function has to be specified more properly. In our next paper this issue will be further elaborated and the corresponding dynamic model investigated in which the economic variables remain non-negative without any nonnegative constraints. Our second conclusion is that the model with continuously distributed time delay exhibits various dynamics including stability, periodic-cycles and aperiodic-cycles, depending on the value of  $m$  as shown in Figure 8.

Next we examine the destabilizing effect when the dynamic system moves to fixed delay from distributed delay. We analytically derive the critical value of the length of the fixed delay at which the stability switch occurs and then numerically demonstrate that increasing the length of the fixed delay from the critical value alters movement of the dynamics from stable steady state, through periodic cycle, to chaos. The simulation result suggests that longer fixed delay induces complex behavior involving chaos more likely. Our third conclusion is essentially the same as our second: there is a period-doubling cascade to chaos if  $\tau$  increases from its critical value  $\tau^*$ .

An important relation between continuously distributed and fixed time delays has been pointed out in this paper. We have shown that the characteristic equation of the distributed case converges to that of the fixed delay model when the shape parameter of the weighting function tends to infinity. This interesting property of the growth model has been also illustrated by the convergence of the stability regions. This means that when the distributed delay becomes more narrowed, cyclic and chaotic behavior are more pronounced. The destabilizing effect can be summarized as follows: time delay could change dynamics significantly implying that the steady state bifurcates to chaos through period-doubling cascade if the length of  $\tau$  increases in the fixed delay model while the same phenomenon occurs if the value of  $m$  increases in the distributed delay model. The main result of this paper is to show the birth of limit cycles and possible chaotic behavior in the continuous-time neoclassical growth model if the delay is taken into account.

## References

- [1] Bischi, G. I., C. Chiarella, M. Kopel and F. Szidarovszky, *Nonlinear Oligopolies: Stability and Bifurcations*, Berlin, Heidelberg, New York, Springer-Verlag, 2010.
- [2] Day, R., "Irregular Growth Cycles," *American Economic Review*, vol. 72, 406-414, 1982.
- [3] Day, R., "The Emergence of Chaos from Classical Economic Growth," *Quarterly Journal of Economics*, vol.98, 203-213, 1983.
- [4] Day, R., *Complex Economic Dynamics: An Introduction to Dynamical Systems and Market Mechanism*, Cambridge, MIT Press, 1994.
- [5] Gandolfo, G., *Economic Dynamics, Study Edition*, Berlin, Heidelberg, New York, Springer-Verlag, 1997.
- [6] Mackey, M. and Glass, L., "Oscillation and Chaos in Physiological Control System," *Science*, vol. 197, 287-289, 1977.
- [7] Jarsulic, M. "Complex Dynamics in a Keynesian Growth Model," *Metroeconomica*, vol. 44, 43-64, 1993.
- [8] Li, T-Y., and J. A. Yorke, "Period Three Implies Chaos," *American Mathematical Monthly*, vol. 82, 985-92, 1975.
- [9] Puu, T., *Attractions, Bifurcations and Chaos: Nonlinear Phenomena in Economics, 2nd Edition*, Berlin, Heidelberg, New York, Springer-Verlag, 2003.
- [10] Rosser, J.B. (Ed.), *Complexity in Economics I, II, III, The International Library of Critical Writings in Economic Series, vol.174*, Edward Elgar, Aldergate, 2004.
- [11] Solow, R., "A Contribution to the Theory of Economic Growth," *Quarterly Journal of Economics*, vol. 70, 65-94, 1956.
- [12] Swan, T., "Economic Growth and Capital Accumulation," *Economic Record*, vol. 32, 334-361,1956.